# An Enhanced Analytical Model of Nonlinear Fiber Effects for Four-Dimensional Symmetric Modulation Formats

Hami Rabbani, Hamid Hossienianfar, Maïté Brandt-Pearce, Senior Member, IEEE

Abstract—Optical transmission systems intrinsically enjoy a four-dimensional (4D) constellation space, corresponding to two quadratures in two polarization states. In this paper, we introduce a general nonlinear model that is valid for 4D symmetric modulation formats. We take the inter-polarization dependency into account to derive this model. The model accounts for all perturbative nonlinear interference (NLI) terms, including self-channel, cross-channel and multi-channel interferences. Split step Fourier simulations show that the proposed model has the ability to predict the NLI with high levels of accuracy for both low and high fiber dispersion regimes. The simulation results further show that previous models, including the EGN model, inaccurately predict the NLI in certain scenarios.

Index Terms—Coherent systems, Enhanced Gaussian noise model, Four-dimensional modulation formats, Gaussian noise model, Kerr nonlinearity, Optical fiber communications.

### I. INTRODUCTION

In coherent fiber-optic communication systems, both quadratures and both polarizations of the electromagnetic field are employed, resulting in a four-dimensional (4D) signal space. Signal disturbance imposed by the Kerr nonlinearity as the signal propagates through an optical fiber is the chief factor limiting the capacity of wavelength division multiplexed (WDM) systems [1]. To counter this limit, nonlinearitytolerant 4D modulation formats have become especially attractive. Optimized modulation formats in a 4D space have been previously studied in [2], [3], irrespective of the nonlinear interference (NLI) that modulation formats undergo during propagation. To find a nonlinearity-resistant constellation, we need a powerful analytical model that enables us to accurately estimate the experienced NLI. This paper presents a model to accurately predict the NLI affecting 4D formats in both low and high fiber dispersion regimes.

Although the literature has a wealth of approximate analytical models for nonlinear fiber propagation [4]–[9], they all focus on estimating the NLI of polarization multiplexed (PM) systems. The first nonlinear model was introduced in 1993 [10]. The Volterra series method, an analytical solution of the nonlinear Schrödinger equation, was presented both in the time and frequency domain in [11]. More recently, the Gaussian noise (GN) model was derived based on the assumption that the transmitted signal in a link approximates

H. Rabbani, H. Hosseinianfar and M. Brandt-Pearce are with the Charles L. Brown Department of Electrical and Computer Engineering, University of Virginia, Charlottesville, VA 22904, USA. E-mails: {dmr3ub, hh9af, mb-p}@virginia.edu.

a Gaussian distribution in dispersion-uncompensated optical systems [6], [12], leading to a slight overestimate of the NLI variance. The first 4D GN-like nonlinear model was introduced in [13]. The original GN models do not include complementary modulation-format-dependant terms. A modulationformat-dependent time domain model was proposed for the first time in [14] by resorting to an asymptotic approximation similar to the far-field approximation in paraxial optics. The authors of [7] found that there is a discrepancy between the time-domain model [14] and the GN model [12]; they attributed this deviation to the Gaussianity assumption of the signal in the GN model. To settle this discrepancy, [7] added a modulation-format-dependent correction term to the cross phase modulation (XPM) estimate. Following the same approach as in [7], the authors of [9] added correction terms to the GN model, taking the self-channel interference (SCI), cross-channel interference (XCI), and multi-channel interference (MCI) terms into account, giving rise to the socalled enhanced Gaussian noise (EGN) model. Comprehensive surveys of nonlinear models proposed up to 2015 and 2020 were given in [15] and [16, Table I], respectively.

All the nonlinear models given in [16, Table I] apply to modulation formats that modulate the two polarizations independently, i.e., 2×2D formats, such as the PM-M-QAM format. However, for 4D formats that modulate all four dimensions jointly, a more general nonlinear model is needed. An analytical model for asymmetric 4D modulation formats was presented in [17], comprising only the SCI. In [18], a 4D nonlinear model able to quantify the impact of SCI (the pink lozenge-shaped island in [9, Fig. 7]) and XPM (the blue lozenge-shaped islands in [9, Fig. 7], named as X1) was derived. The model in [18] is only able to estimate the impact of NLI in high dispersion systems because it discards XCI (except for XPM) and MCI terms. No one has as yet ascertained how to estimate the XCI (the islands marked as X2, X3, and X4 in [9, Fig. 7]) and MCI (the islands marked as M0, M1, M2, M3, and M4 in [9, Fig. 7]) terms that disturb 4D constellations.

This paper is an extension of [18] providing a far more thorough and complete approach to deriving the NLI terms, such as SCI, XCI and MCI, by taking the interpolarization dependency into consideration. Unlike the model presented in [18] that applies only to high dispersion fiber systems, this work accurately models the nonlinear interference in various scenarios, including narrow bandwidth channels often encountered in elastic optical networks and transmission over

low dispersion fiber. To the best of our knowledge, it is the first paper that presents a comprehensive solution to modeling the NLI that is applicable to any system using a 4D modulation format. The reader may want to use the proposed model for a wide range of purposes, such as quality of transmission estimation or new modulation format design.

The structure of the paper is as follows. In Sec. II, we deal with the Manakov equation in the pseudolinear regime, where the SNR is high enough to support the first order perturbation approach. Sec. III presents the key result of this work, the new NLI model. Sec. IV is devoted to numerical results showing how various 4D constellations compare in terms of the experienced NLI. Sec. V provides the conclusion. The paper ends with an appendix, where the derivation of the key result is given in detail.

Notation:  $(\cdot)_x$  and  $(\cdot)_y$  are used throughout this paper to denote variables associated to polarizations x and y, respectively. The boldface symbols stand for two dimensional complex functions [18, Eq. (1)]. Expectations are shown by  $\mathbb{E}\{\cdot\}$ , and  $(\cdot)^{\dagger}$  stands for the complex conjugate.

### II. PRELIMINARIES

Let us start with the Manakov equation [19, Eq. (2)], [18, Eq. (2)]<sup>1</sup>,

$$\frac{\partial}{\partial z} \boldsymbol{u}(t,z) = -\frac{i\beta_2}{2} \frac{\partial^2}{\partial t^2} \boldsymbol{u}(t,z) 
+ i\frac{8}{9} \gamma f(z) \boldsymbol{u}^{\dagger}(t,z) \boldsymbol{u}(t,z) \boldsymbol{u}(t,z), \qquad (1)$$

where u(t,z) is linked to the electrical field E(t,z) [18, Eq. (1)] through a distance-dependent scaling function, compensating for gain/loss, as in [14, Sec. II], [18, Eq. 2]. In (1),  $\beta_2$  is the group velocity dispersion, f(z) is the loss/gain power profile, and  $\gamma$  is the fiber nonlinearity coefficient. The function f(z) is equivalent to  $f(z) = \exp\{-\alpha \operatorname{mod}(z,L)\}$  for lumped amplification, where  $\alpha$  is the loss coefficient, L is the span length and  $\operatorname{mod}(z,L)$  indicates the distance between the point z and the nearest preceding amplifier.

We express the linear solution to (1) as [7, Eq. (1)]

$$\mathbf{u}(t,z) = \sum_{n=1}^{N} \sum_{k} e^{-i\nu_n t + \frac{i\beta_2 \nu_n^2}{2} z} \mathbf{a}_{n,k} g_n(t - kT_n - \beta_2 \nu_n z, z),$$
(2)

where  $\nu_n$  is the central frequency of channel n and  $a_{n,k} = [a_{n,k,x} \ a_{n,k,y}]^{\mathrm{T}}$  is a column vector comprising two elements representing the k-th symbol transmitted by channel n. Eq. (2) is an extension of [7, Eq. (1)], [18, Eq. (3)] when the WDM spectrum is occupied by N channels whose bandwidths are allowed to differ from each other. The dispersed pulse waveform at point z along the fiber is  $g_n(t,z) = \exp(-iz\beta_2\partial_t^2/2)g_n(t,0)$  [20], where  $g_n(t,0)$  is the injected waveform in channel n, and  $\partial_t$  is the time derivative operator. The symbol rate of channel n is given by  $T_n^{-1}$ . In this paper, we denote n as the channel of interest (COI).

We would like to detect the zeroth symbol in the COI, namely  $a_{n,0}$ , with no loss of generality. The COI is matched filtered with a filter whose impulse response is proportional to  $g_n^*(t,L)$  [7]. The extracted symbol at the receiver may be expressed as  $a_{n,0} + \Delta a_{n,0}$ , where  $\Delta a_{n,0}$  accounts for the NLI. By resorting to the perturbation approach, the NLI contribution  $\Delta a_{n,0}$  that yields a first order solution of the Manakov equation can be written as [7, Eqs. (3)-(5)], [20, Eq. (3)], [18, Eq. (4)]

$$\Delta \boldsymbol{a}_{n,0} = i \frac{8}{9} \gamma \sum_{n_1, n_2, n_3 \in \mathcal{T}} \sum_{h, k, l} \boldsymbol{a}_{n_2, k}^{\dagger} \boldsymbol{a}_{n_1, h} \boldsymbol{a}_{n_3, l} H_{n_1, n_2, n_3}(h, k, l),$$
(3)

where 
$$\mathcal{T} = \left\{ (n_1, n_2, n_3) \in \{1, \cdots, N\}^3 \right\}$$
, and

$$\begin{split} H_{n_{1},n_{2},n_{3}}(h,k,l) = & \int_{0}^{L} \mathrm{d}z \int_{-\infty}^{\infty} \mathrm{d}t f(z) \\ & \cdot g_{n}^{*}(t-\beta_{2}\nu_{n}z,z) \mathrm{e}^{i\nu_{n}t} \mathrm{e}^{-i\frac{\beta_{2}}{2}(\nu_{n})^{2}z} \\ & \cdot g_{n_{2}}^{*}(t-kT_{n_{2}}-\beta_{2}\nu_{n_{2}}z,z) \mathrm{e}^{i\nu_{n_{2}}t} \mathrm{e}^{-i\frac{\beta_{2}}{2}(\nu_{n_{2}})^{2}z} \\ & \cdot g_{n_{1}}(t-hT_{n_{1}}-\beta_{2}\nu_{n_{1}}z,z) \mathrm{e}^{-i\nu_{n_{1}}t} \mathrm{e}^{i\frac{\beta_{2}}{2}(\nu_{n_{1}})^{2}z} \\ & \cdot g_{n_{3}}(t-lT_{n_{3}}-\beta_{2}\nu_{n_{3}}z,z) \mathrm{e}^{-i\nu_{n_{3}}t} \mathrm{e}^{i\frac{\beta_{2}}{2}(\nu_{n_{3}})^{2}z}. \end{split}$$

Note that  $H(\cdot)$  defined above and other expressions resulting from it defined below  $(S(\cdot), \chi_1(\cdot), \text{ etc.})$  depend on n, but for notational compactness we suppressed the dependence on n throughout the paper.

Eq. (3) is a generalization of [7, Eq. (5)], [20, Eq. (3)], [18, Eq. (4)] for a multi-channel WDM system. Considering  $g(t,z)=\int \mathrm{d}w \tilde{g}(w) \exp(-iwt+iw^2\beta_2z/2)/(2\pi)$ , where  $\tilde{g}(w)$  is the Fourier transform of g(t,0) (see [20, Appendix] and [19, Eqs. (31) and (34)]), (4) is expressed in the frequency domain as

$$H_{n_1,n_2,n_3}(h,k,l) = \int \frac{\mathrm{d}^3 w}{(2\pi)^3} S_{n_1,n_2,n_3}(w_1, w_2, w_3) \cdot e^{i(w_1 h T_{n_1} - w_2 k T_{n_2} + w_3 l T_{n_3})},$$
 (5)

respectively, where  $\int d^3w$  stands for  $\int \int \int dw_1 dw_2 dw_3$ , and

$$S_{n_1,n_2,n_3}(w_1, w_2, w_3) = \tilde{g}_n^*(w_1 - w_2 + w_3 - \nu_n) \cdot \tilde{g}_{n_1}(w_1 - \nu_{n_1}) \tilde{g}_{n_2}^*(w_2 - \nu_{n_2}) \tilde{g}_{n_3}(w_3 - \nu_{n_3}) \Upsilon(w_1, w_2, w_3),$$
(6)

and

$$\Upsilon(w_1, w_2, w_3) = \int_0^L dz f(z) e^{i\beta_2(w_2 - w_3)(w_2 - w_1)z}$$
 (7)

is the link function.

### III. THE KEY RESULT: NLI VARIANCE

This section provides the key result of this work, which is the power of the NLI contribution given in (3). The reader can find a detailed derivation of the key result in the Appendix. To obtain our result, we will make the same assumptions as described in [18, Sec. III].

Channels across the spectrum can have different launch powers and different 4D modulation formats. The launch

<sup>&</sup>lt;sup>1</sup>We note that in this paper we neglect the nonlinear interactions between signal and amplified spontaneous emission noise.

powers in the x- and y-polarization are assumed to be the same, which means that

$$\frac{P_n}{2} = \mathbb{E}\{|a_{n,x}|^2\} = \mathbb{E}\{|a_{n,y}|^2\},\tag{8}$$

where  $P_n$  is the total launch power transmitted in channel n. The power of the NLI on channel n is related to (3) as<sup>2</sup>

$$P_{\text{NLI},n} = \text{trace} \left[ \text{Cov} \left\{ \Delta \boldsymbol{a}_{n,0} \right\} \right]$$

$$= \sigma_{\text{NLI},n,x}^2 + \sigma_{\text{NLI},n,y}^2,$$
(10)

where  $\sigma_{\text{NLI},n,x}^2$  and  $\sigma_{\text{NLI},n,y}^2$  are the NLI variances on polarizations x and y, respectively. The NLI variance on polarization x (and similarly y) can be written as

$$\sigma_{\text{NLI},n,x}^{2} = \frac{64}{81} \gamma^{2} \sum_{n_{1},n_{2},n_{3} \in \mathcal{T}} P_{n_{1},x} P_{n_{2},x} P_{n_{3},x} \cdot \left( \delta_{n_{1},n_{2}} \delta_{n_{1},n_{3}} \Psi_{1} \chi_{1} + \delta_{n_{1},n_{2}} \Psi_{2} \chi_{2} + \delta_{n_{1},n_{3}} \Psi_{3} \chi_{3} + 3Z \right),$$
(11)

where  $P_{n_i,x}$  is the launch power of channel  $n_i$  transmitted in polarization x. The terms  $\chi_1$ ,  $\chi_2$ ,  $\chi_3$ , and Z are given in Table I, while  $\Psi_1$ ,  $\Psi_2$ ,  $\Psi_3$  are expressed in Table II. By swapping x and y in (11) and in the terms expressed in Table II, the NLI variance in the y polarization  $\sigma^2_{\text{NLI},n,y}$  can be readily obtained from (11).

Intuitively, the product  $\delta_{n_1,n_2}\delta_{n_1,n_3}$  in (11) means that the frequency components  $w_1$ ,  $w_2$ ,  $w_3$ , given in (6), are within a single channel. The term  $\delta_{n_1,n_2}$ , on the other hand, implies that the frequency components  $w_1$  and  $w_2$  are located in the same channel. The same interpretation is true for  $\delta_{n_1,n_3}$  in (11). As shown in [18, Sec. III], the terms  $\Psi_1$ ,  $\Psi_2$ , and  $\Psi_3$  converge to the EGN model in the special case of independent polarizations. We can call the integral terms  $\chi_2$  and  $\chi_3$  the fourth order noise coefficients, like [20, Eq. (16)]. The terms  $\chi_1$  and Z are therefore called the sixth order and second order noise coefficients (see [20, Eq. (13)]), respectively.

### IV. NUMERICAL RESULTS

In this section, we validate our proposed derived NLI power (10) with split-step Fourier method (SSFM) simulations in a single-link scenario for a number of modulation formats chosen from [21] by mapping the first two coordinates to the x polarization and the last two to the y polarization. We compare the 4D modulation formats in terms of

$$\eta_n = \frac{P_{\text{NLI},n}}{P^3},\tag{12}$$

where  $P_{\text{NLI},n}$  is the NLI power at the COI. We also assume in (12) that  $P = P_{n_1} = P_{n_2} = P_{n_3}$ . In (12),  $\eta_n$  is the NLI noise experienced by channel n normalized over  $P^{-3}$ , and so it is independent of the launch power per channel.

In our simulations, we consider two scenarios that are quite distinct from each other, like in [22]. The first and second scenarios use standard single mode fiber (SMF) and non-zero dispersion shifted fiber (NZDSF), respectively. Both scenarios operate over 100-km uniform spans. We also assume that the

 $\label{eq:Table I} \mbox{Table I} \\ \mbox{Integral expressions for the terms used in (11)}.$ 

Term	Integral Expression
$\chi_1(n_1,n_2,n_3)$	$\frac{1}{T_{n_1}} \int \frac{\mathrm{d}^3 w}{(2\pi)^3} \frac{\mathrm{d}^2 w'}{(2\pi)^2} S_{n_1, n_2, n_3}(w_1, w_2, w_3)$
	$\cdot S_{n_1,n_2,n_3}^*(w_1',w_2',w_1+w_3+w_2'-w_2-w_1')$
$\chi_2(n_1,n_2,n_3)$	$\frac{1}{T_{n_1}T_{n_3}} \int \frac{\mathrm{d}^3 w}{(2\pi)^3} \frac{\mathrm{d}w_2'}{2\pi} S_{n_1,n_2,n_3}(w_1,w_2,w_3)$
	$S_{n_1,n_2,n_3}^*(w_1 - w_2 + w_2', w_2', w_3)$
$\chi_3(n_1,n_2,n_3)$	$\frac{1}{T_{n_1}T_{n_2}} \int \frac{\mathrm{d}^3 w}{(2\pi)^3} \frac{\mathrm{d} w_2'}{2\pi} S_{n_1,n_2,n_3}(w_1, w_2, w_3)$
	$\cdot S_{n_1, n_2, n_3}^*(w_1', w_2, w_1 + w_3 - w_1')$
$Z(n_1, n_2, n_3)$	$\frac{1}{T_{n_2}T_{n_1}T_{n_3}} \int \frac{\mathrm{d}^3 w}{(2\pi)^3}  S_{n_1,n_2,n_3}(w_1,w_2,w_3) ^2$

Table II The terms used in (11). The values of  $\varphi_1,\cdots,\varphi_5$  are given in Table III.

Term	Expression
$\Psi_1$	$\varphi_1 - 12\varphi_2 + 2\varphi_3 + \varphi_4 - 12\varphi_5 + 24$
$\Psi_2$	$5\varphi_2 + 5\varphi_5 - 15$
$\Psi_3$	$\varphi_2 + \varphi_5 - 3$

Table III Expressions for the terms  $\varphi_1,\cdots,\varphi_5$  used in Table II.

Term	Term Expression		Expression	
$\varphi_1$	$\frac{\mathbb{E}\{ a_{n_1,\mathbf{X}} ^6\}}{\mathbb{E}^3\{ a_{n_1,\mathbf{X}} ^2\}}$	$\varphi_2$	$\frac{\mathbb{E}\{ a_{n_1,\mathbf{X}} ^4\}}{\mathbb{E}^2\{ a_{n_1,\mathbf{X}} ^2\}}$	
$\varphi_3$	$\left  \frac{\mathbb{E}\{ a_{n_1,\mathbf{X}} ^4 a_{n_1,\mathbf{Y}} ^2\}}{\mathbb{E}^3\{ a_{n_1,\mathbf{X}} ^2\}} \right $	$\varphi_4$	$\frac{\mathbb{E}\{ a_{n_1,\mathbf{y}} ^4 a_{n_1,\mathbf{x}} ^2\}}{\mathbb{E}^3\{ a_{n_1,\mathbf{x}} ^2\}}$	
$\varphi_5$	$\frac{\mathbb{E}\{ a_{n_1,\mathbf{X}} ^2 a_{n_1,\mathbf{y}} ^2\}}{\mathbb{E}^2\{ a_{n_1,\mathbf{X}} ^2\}}$			

WDM spectrum in both scenarios accommodates either 50 Gbaud channels with 50 GHz frequency spacing or 20 Gbaud channels with 20 GHz spacing. We consider the following parameters in our setup for SMF or NZDSF, respectively: dispersion coefficient D=16.5 or 3.8 ps/nm/km, nonlinear coefficient  $\gamma=1.3$  or 1.5 1/W/km, and attenuation  $\alpha=0.2$  dB/km in both cases. wavelength is 1550 nm.

Finding a numerical solution to the Manakov equation is a big challenge faced by scientists today. This is caused by high memory requirements and the excessive need for very large fast Fourier transforms. The SSFM simulation (and the corresponding analytical models) were therefore limited to a fully occupied bandwidth of 0.5 THz similar to [18, Sec. IV]. Four modulation formats, including PM-QPSK, subset optimized PM-QPSK (SO-PM-QPSK) [21], [23], PM-16QAM and a4\_256 [21], [24] were simulated. The figures show  $\eta_n$  in dB( $W^{-2}$ ) =  $10\log_{10}(\eta_n \cdot 1W^2)$  as a function of channel number n.

Fig. 1 gives information about the NLI that 4D constellations have undergone after traveling through SMF. As can be

<sup>&</sup>lt;sup>2</sup>Under the assumptions made in [18, Sec. III], the non-diagonal terms of the covariance matrix are zero.

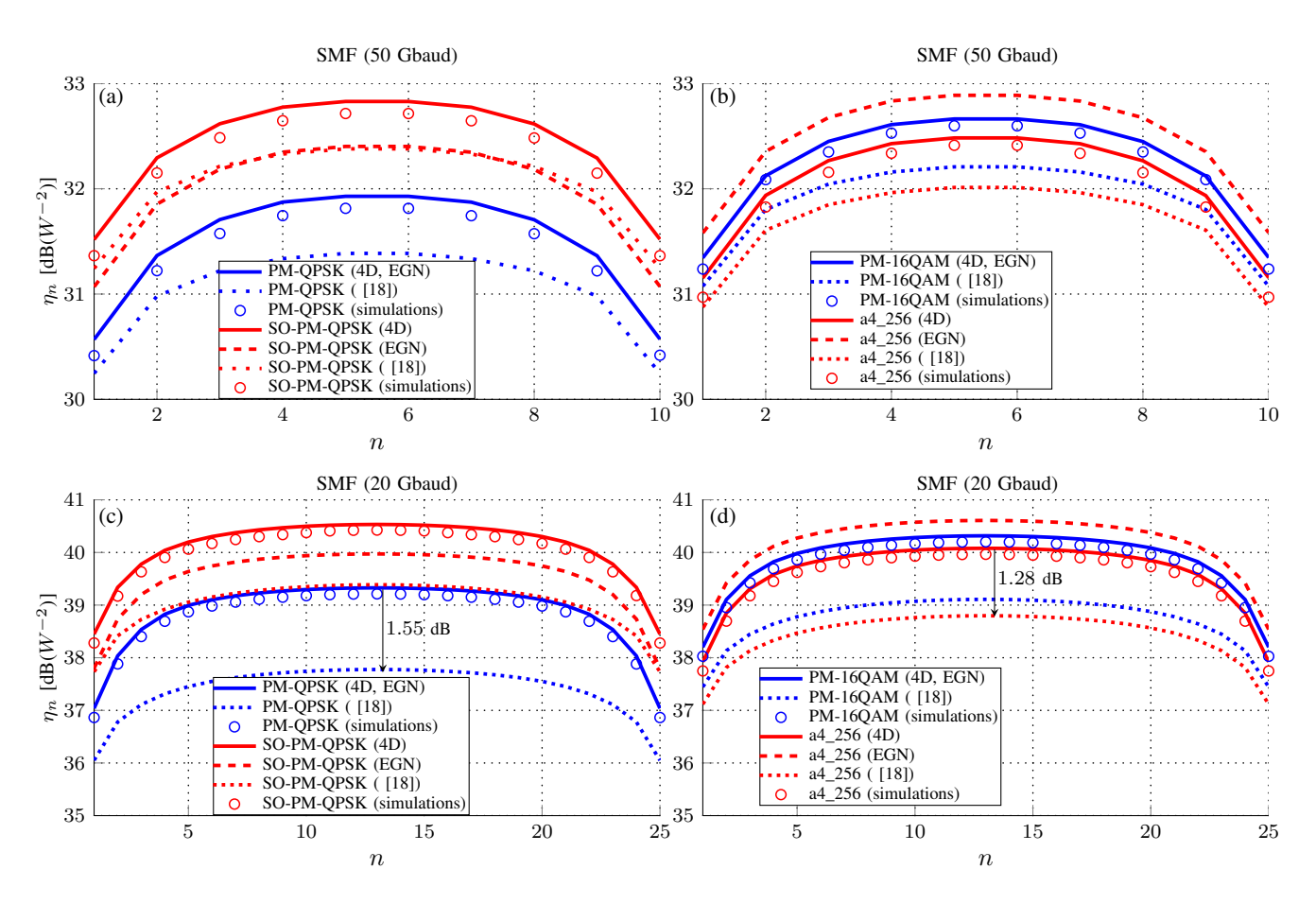


Figure 1.  $\eta_n$  as a function of channel number n after 5 spans of SMF fiber, comparing different models; the proposed model is referred to as '4D'. In the top panel (Figs. (a) and (b)) the SMF supports N=10 WDM channels with symbol rate 50 Gbaud and channel spacing 50 GHz, whereas in the bottem panel (Figs. (c) and (d)) SMF supports N=25 channels with symbol rate 20 Gbaud and channel spacing 20 GHz.

seen in Fig. 1, the results obtained from our model match SSFM simulations, while the EGN model does not accurately predict the NLI of SO-PM-QPSK and a4\_256 formats. The EGN model underestimates the NLI of 16-point constellations (Figs. 1 (a) and (c)), while for 256-point constellations, it overestimates the NLI (Figs. 1 (b) and (d)). Figs. 1 (a) and (b) show the results for high symbol rates, where the predominant nonlinear terms are SCI and XPM terms. Figs. 1 (c) and (d), on the other hand, illustrate the results for low symbol rates in which the major NLI contribution comes from MCI terms. As indicated in Figs. 1 (c) and (d), the results obtained using our model follow SSFM simulations very closely since our model fully accounts for all the NLI terms. The model given in [18, Eq. (15)] departs significantly from SSFM simulations because it neglects MCI terms. The gap between our model and the model given in [18, Eq. (15)] becomes greater in systems operating at low baud rates: up to 1.55 dB and 1.28 dB for PM-QPSK and a4\_256 modulation formats, respectively, as shown in Figs. 1 (c) and (d).

We plot corresponding numerical results for NZDSF in Fig. 2 to evidence how our model is also suitable for estimating the NLI for different fiber types [22]. In each of the figures shown in Fig. 2, the results obtained through our model are in close agreement with SSFM simulation results. The model presented in [18] substantially underestimates the NLI,

especially for the narrower band signals shown in Figs. 2 (c) and (d), due mostly to the massive number of discarded MCI terms, in addition to low dispersion in NZDSF. As can be seen in Fig. 2 (c), the NLI results of [18] are below the SSFM results by about 3.46 dB for PM-QPSK and by about 2.40 dB for SO-PM-PQSK. Fig. 2 (d) shows that the deviation between the SSFM and the NLI model results of [18] is about 2.73 dB for a4\_256. This gap for PM-16QAM is about 2.55 dB.

Results show that our NLI model can accurately predict the NLI for various bandwidth signals, unlike the model in [18] that is accurate only for large signal bandwidths. Furthermore, our model has the ability to predict the NLI of systems using low dispersion fiber, such as NZDSF, resulting in high NLI; the model presented in [18] fails to provide an accurate estimate of the impairments in these cases. Our results are analogous to [22, Fig. 1], which demonstrates that for a fully loaded link of SMF or NZDSF, the MCI contributions to the NLI become more significant for symbol rates lower than around 25 Gbaud and 50 Gbaud, respectively. As the symbol rate decreases, we face a huge number of MCI terms whose computation is a considerable challenge. To circumvent this issue, we follow an approach similar to [25, Fig. 1], meaning that many terms in (11) that are repetitive are not recomputed. Our model can be used for a wide range of purposes, such as reducing a constellation's vulnerability to NLI. The discrepancy between PREPRINT, NOVEMBER 27, 2023 5

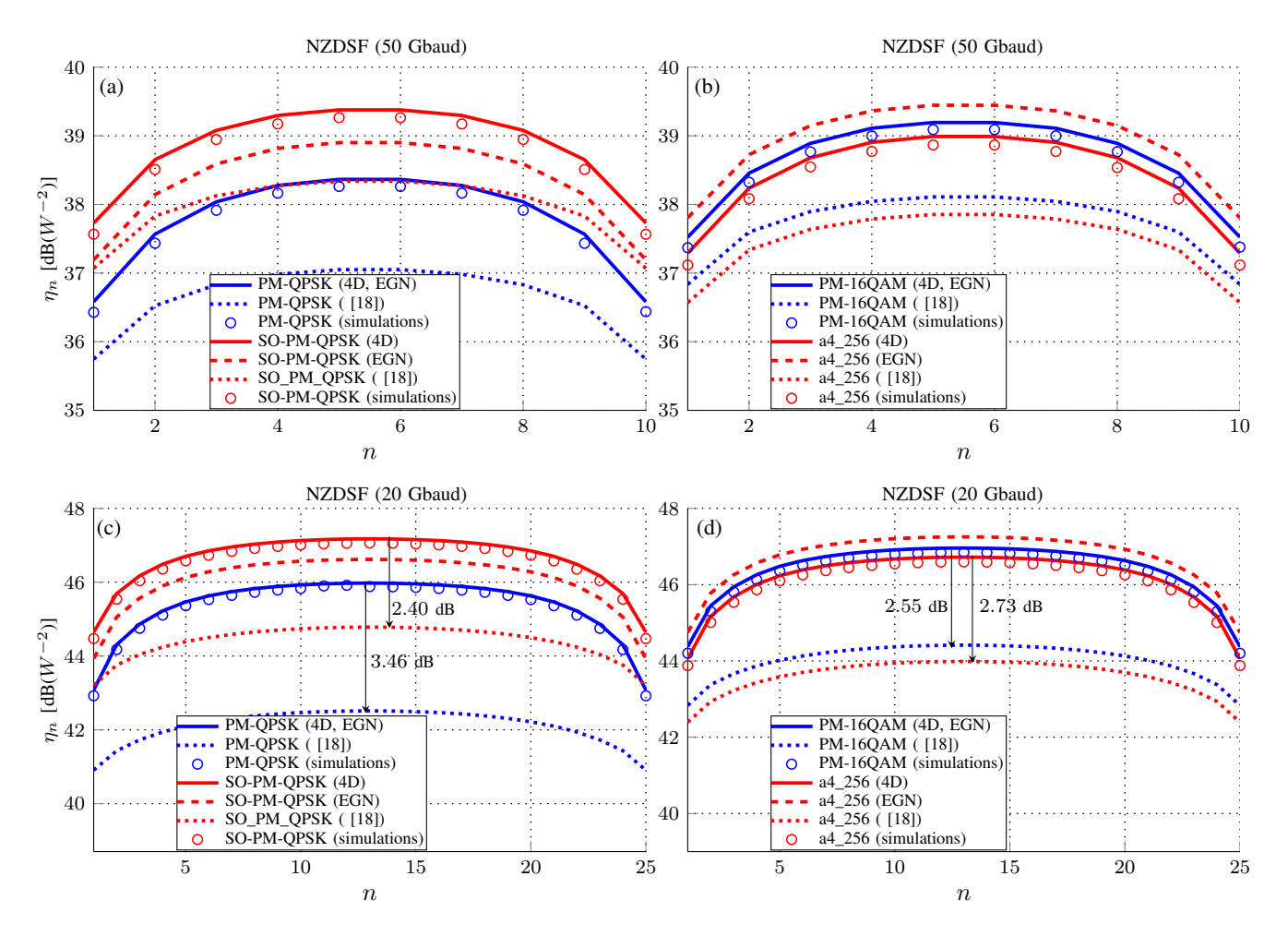


Figure 2.  $\eta_n$  as a function of channel number n after 5 spans of NZDSF fiber, comparing different models; the proposed model is referred to as '4D'. In the top panel (Figs. (a) and (b)) the NZDSF supports N=10 WDM channels with symbol rate 50 Gbaud and channel spacing 50 GHz, whereas in the bottem panel (Figs. (c) and (d)) NZDSF supports N=25 channels with symbol rate 20 Gbaud and channel spacing 20 GHz.

SSFM simulations and the results obtained using our 4D model is on average 0.14 dB for the modulation formats and system scenarios tested.

## V. CONCLUSION

A detailed derivation of an analytical model for the nonlinear fiber interference experienced by signals using 4D modulation formats was given. The derived model has the power to quantify the impact of all the NLI terms, such as SCI, XCI, and MCI terms on a 4D signal space. The previously-proposed GN and EGN models ignore the interpolarization dependency that the proposed model captures. The proposed model is accurate for a variety of scenarios, including both small and large bandwidth signals and both high and low dispersion fiberbased systems. Our model results in an average error of a small fraction of a dB, while other models result in errors of 2-3 dB for typical scenarios.

### VI. ACKNOWLEDGMENT

This work was supported in part by NSF grant CNS-1718130.

# VII. APPENDIX

The aim of this section is to derive the NLI variance of polarization x, given in (10). We set out with the x-polarized component of (3), which is

$$\Delta a_{n,0,x} = i\frac{8}{9}\gamma \sum_{n_1,n_2,n_3 \in \mathcal{T}} \sum_{h,k,l} H_{n_1,n_2,n_3}(h,k,l) \cdot \left( a_{n_1,h,x} a_{n_2,k,x}^* a_{n_3,l,x} + a_{n_1,h,y} a_{n_2,k,y}^* a_{n_3,l,x} \right).$$
(13)

Under the assumption that the modulation formats are zero-mean and symmetric in the complex plane, we have  $\mathbb{E}\{a_{n_1,h,x}\}=\mathbb{E}\{a_{n_1,h,x}^*\}=0$ ,  $\mathbb{E}\{a_{n_1,h,x}a_{n_1,h',x}\}=0$ ,  $\mathbb{E}\{a_{n_1,h,x}a_{n_1,h',x}^*\}=0$ ,  $\mathbb{E}\{a_{n_1,h,x}a_{n_1,h',y}^*\}=\mathbb{E}\{a_{n_1,h,x}^*a_{n_1,h',y}^*\}=0$ ,  $\mathbb{E}\{|a_{n_1,h,x}|^2a_{n_1,h',x}\}=\mathbb{E}\{|a_{n_1,h,x}|^2a_{n_1,h',y}\}=0$ , and  $\mathbb{E}\{a_{n_1,h,x}a_{n_1,h',x}^*\}=\mathbb{E}\{|a_{n_1,x}|^2\}\delta_{h,h'}$  (see [19, Appendix A], [18, Appendix A]). The variance of (13) is equal to

$$\sigma_{\text{NLI},n,x}^2 = \mathbb{E}\{\Delta a_{n,0,x} \Delta a_{n,0,x}^*\} - \mathbb{E}\{\Delta a_{n,0,x}\} \mathbb{E}\{\Delta a_{n,0,x}^*\},$$
(14)

	7	Γable	IV		
EXPRESSIONS	FOR	THE	TERMS	USED	IN (18).

Term	Expression
$A_1$	$\frac{64}{81}\gamma^2 \sum_{h,k,l,h',k',l} H_{n_1,n_1,n_1}(h,k,l) H_{n_1,n_1,n_1}^*(h',k',l') \mathbb{E}\{a_{n_1,h,\mathbf{x}}a_{n_1,k,\mathbf{x}}^* a_{n_1,l,\mathbf{x}}a_{n_1,h',\mathbf{x}}^* a_{n_1,k',\mathbf{x}}a_{n_1,l',\mathbf{x}}^*\}$
$A_2$	$ \frac{64}{81} \gamma^2 \sum_{h,k,l,h',k',l} H_{n_1,n_3,n_3}(h,k,l) H_{n_1,n_3,n_3}^*(h',k',l') \mathbb{E}\{a_{n_1,h,\mathbf{x}} a_{n_1,h',\mathbf{x}}^*\} \mathbb{E}\{a_{n_3,k,\mathbf{x}}^* a_{n_3,l',\mathbf{x}} a_{n_3,l',\mathbf{x}}^* a_{n_3,l',\mathbf{x}} \} $
$A_3$	$ \frac{64}{81} \gamma^2 \sum_{h,k,l,h',k',l} H_{n_1,n_3,n_3}(h,k,l) H_{n_3,n_3,n_1}^*(h',k',l') \mathbb{E}\{a_{n_1,h,\mathbf{x}} a_{n_1,l',\mathbf{x}}^*\} \mathbb{E}\{a_{n_3,k,\mathbf{x}}^* a_{n_3,l,\mathbf{x}} a_{n_3,h',\mathbf{x}}^* a_{n_3,k',\mathbf{x}}\} $
$A_4$	$ \begin{vmatrix} \frac{64}{81} \gamma^2 \sum_{h,k,l,h',k',l} H_{n_1,n_2,n_1}(h,k,l) H_{n_1,n_2,n_1}^*(h',k',l') \mathbb{E}\{a_{n_2,k,\mathbf{x}}^* a_{n_2,k',\mathbf{x}}\} \mathbb{E}\{a_{n_1,h,\mathbf{x}} a_{n_1,h',\mathbf{x}}^* a_{n_1,l,\mathbf{x}} a_{n_1,l',\mathbf{x}}^*\} \end{vmatrix} $
$A_5$	$ \frac{64}{81} \gamma^2 \sum_{h,k,l,h',k',l} H_{n_1,n_1,n_3}(h,k,l) H_{n_3,n_1,n_1}^*(h',k',l') \mathbb{E}\{a_{n_3,l,\mathbf{x}} a_{n_3,h',\mathbf{x}}^*\} \mathbb{E}\{a_{n_1,h,\mathbf{x}} a_{n_1,k',\mathbf{x}}^* a_{n_1,l',\mathbf{x}} \} $
$A_6$	$ \frac{64}{81} \gamma^2 \sum_{h,k,l,h',k',l} H_{n_1,n_1,n_3}(h,k,l) H_{n_1,n_1,n_3}^*(h',k',l') \mathbb{E}\{a_{n_3,l,\mathbf{x}} a_{n_3,l',\mathbf{x}}^*\} \mathbb{E}\{a_{n_1,h,\mathbf{x}} a_{n_1,k,\mathbf{x}}^* a_{n_1,h',\mathbf{x}}^* a_{n_1,h',\mathbf{x}} a_{n_1,k',\mathbf{x}}\} $
$A_7$	$\begin{bmatrix} \frac{64}{81} \gamma^2 \sum_{h,k,l,h',k',l} H_{n_1,n_2,n_3}(h,k,l) H_{n_1,n_2,n_3}^*(h',k',l') \mathbb{E}\{a_{n_1,h,x} a_{n_1,h',x}^*\} \mathbb{E}\{a_{n_2,k,x}^* a_{n_2,k',x}\} \mathbb{E}\{a_{n_3,l,x} a_{n_3,l',x}^*\} \end{bmatrix}$
$A_8$	$\begin{bmatrix} \frac{64}{81} \gamma^2 \sum_{h,k,l,h',k',l} H_{n_1,n_2,n_3}(h,k,l) H_{n_3,n_2,n_1}^*(h',k',l') \mathbb{E}\{a_{n_1,h,\mathbf{x}} a_{n_1,l',\mathbf{x}}^*\} \mathbb{E}\{a_{n_2,k,\mathbf{x}}^* a_{n_2,k',\mathbf{x}}\} \mathbb{E}\{a_{n_3,l,\mathbf{x}} a_{n_3,h',\mathbf{x}}^*\} \end{bmatrix}$

where the expectation terms  $\mathbb{E}\{\Delta a_{0,x}\}$  and  $\mathbb{E}\{\Delta a_{0,x}^*\}$  are therefore zero. Substituting (13) into (14) gives

$$\sigma_{\text{NLI},n,x}^{2} = \frac{64}{81} \gamma^{2} \sum_{n_{1},n_{2},n_{3} \in \mathcal{T}} \sum_{n'_{1},n'_{2},n'_{3} \in \mathcal{T}} \sum_{h,k,l,h',k',l'} H_{n_{1},n_{2},n_{3}}(h,k,l) H_{n'_{1},n'_{2},n'_{3}}^{*}(h',k',l') \cdot \left( \mathbb{E}\{a_{n_{1},h,x}a_{n_{2},k,x}^{*}a_{n_{3},l,x}a_{n'_{1},h',x}^{*}a_{n'_{2},k',x}a_{n'_{3},l',x}^{*}\} + \mathbb{E}\{a_{n_{1},h,x}a_{n_{2},k,x}^{*}a_{n_{3},l,x}a_{n'_{1},h',y}^{*}a_{n'_{2},k',y}a_{n'_{3},l',x}^{*}\} + \mathbb{E}\{a_{n_{1},h,y}a_{n_{2},k,y}^{*}a_{n_{3},l,x}a_{n'_{1},h',x}^{*}a_{n'_{2},k',x}a_{n'_{3},l',x}^{*}\} + \mathbb{E}\{a_{n_{1},h,y}a_{n_{2},k,y}^{*}a_{n_{3},l,x}a_{n'_{1},h',y}^{*}a_{n'_{2},k',y}a_{n'_{3},l',x}^{*}\} \right).$$
 (15)

To compute (15), four terms must be calculated, expressed as

$$\sigma_{\text{NLI},n,x}^{2} = \sigma_{\text{NLI},n,x,1\text{st}}^{2} + \sigma_{\text{NLI},n,x,2\text{nd}}^{2} + \sigma_{\text{NLI},n,x,3\text{rd}}^{2} + \sigma_{\text{NLI},n,x,4\text{th}}^{2},$$
(16)

where  $\sigma_{\text{NLI},n,\text{x,1st}}^2$ ,  $\sigma_{\text{NLI},n,\text{x,2nd}}^2$ ,  $\sigma_{\text{NLI},n,\text{x,3rd}}^2$ , and  $\sigma_{\text{NLI},n,\text{x,4th}}^2$  are the first, second, third, and fourth term of (15), respectively. We only give the procedure for calculating  $\sigma_{\mathrm{NLI},n,\mathbf{x},1\mathrm{st}}^2$  in detail, and the others can be derived following the same approach.

Given the bias terms described in [14, Sec. VIII, Eqs. (63)– (67)], [7, Sec. 3, Eq. (17)], [9, Appendix A], [26, Sec.IV-B and the text after (63)], [6, Appendix C]) and [18, Eq. (37)], we must ignore the triplets (h, k, l) in which h = k or k = l. The following cases should therefore be taken into account for computing  $\sigma_{\text{NLI},n,x,1\text{st}}^2$ :

1) 
$$n_1 = n_2 = n_3 = n'_1 = n'_2 = n'_3$$
  
2)  $n_1 = n'_1 \neq n_2 = n_3 = n'_2 = n'_3$   
3)  $n_1 = n'_3 \neq n_2 = n_3 = n'_1 = n'_2$   
4)  $n_2 = n'_2 \neq n_1 = n_3 = n'_1 = n'_3$   
5)  $n_3 = n'_1 \neq n_1 = n_2 = n'_2 = n'_3$   
6)  $n_3 = n'_3 \neq n_1 = n_2 = n'_1 = n'_2$   
7)  $n_1 = n'_1 \neq n_2 = n'_2 \neq n_3 = n'_3$   
8)  $n_1 = n'_3 \neq n_2 = n'_2 \neq n_3 = n'_1$ ,

2) 
$$n_1 = n'_1 \neq n_2 = n_3 = n'_2 = n'_3$$

3) 
$$n_1 = n_3' \neq n_2 = n_3 = n_1' = n_2'$$

4) 
$$n_2 = n_2' \neq n_1 = n_3 = n_1' = n_2'$$

5) 
$$n_3 = n'_1 \neq n_1 = n_2 = n'_2 = n'_3$$

6) 
$$n_3 = n'_3 \neq n_1 = n_2 = n'_1 = n'_2$$

7) 
$$n_1 = n'_1 \neq n_2 = n'_2 \neq n_3 = n'_3$$

8) 
$$n_1 = n'_3 \neq n_2 = n'_2 \neq n_3 = n'_1$$
,

resulting in

$$\sigma_{\text{NLI},n,x,1st}^{2} = \frac{64}{81} \gamma^{2} \sum_{n_{1},n_{2},n_{3} \in \mathcal{T}} \sum_{n'_{1},n'_{2},n'_{3} \in \mathcal{T}} \sum_{h,k,l,h',k',l'} \sum_{H_{n_{1},n_{2},n_{3}}(h,k,l) H_{n'_{1},n'_{2},n'_{3}}(h',k',l')} \cdot \left( \delta_{n_{1},n_{3}} \delta_{n_{1},n_{2}} \delta_{n_{1},n'_{1}} \delta_{n_{2},n'_{2}} \delta_{n_{3},n'_{3}} \right. \\ \cdot \mathbb{E} \left\{ a_{n_{1},h,x} a_{n_{1},k,x}^{*} a_{n_{1},l,x} a_{n_{1},h',x}^{*} a_{n_{1},k',x} a_{n_{1},l',x} \right\} \\ + \delta_{n_{2},n_{3}} \bar{\delta}_{n_{1},n_{3}} \delta_{n_{1},n'_{1}} \delta_{n_{2},n'_{2}} \delta_{n_{3},n'_{3}} \mathbb{E} \left\{ a_{n_{1},h,x} a_{n_{1},h',x}^{*} \right\} \\ \cdot \mathbb{E} \left\{ a_{n_{3},k,x}^{*} a_{n_{3},l,x} a_{n_{3},k',x} a_{n_{3},l',x}^{*} \right\} \\ + \delta_{n_{2},n_{3}} \bar{\delta}_{n_{1},n_{3}} \delta_{n_{1},n'_{3}} \delta_{n_{2},n'_{2}} \delta_{n_{3},n'_{1}} \mathbb{E} \left\{ a_{n_{1},h,x} a_{n_{1},l',x}^{*} \right\} \\ \cdot \mathbb{E} \left\{ a_{n_{3},k,x}^{*} a_{n_{3},l,x} a_{n_{3},h',x}^{*} a_{n_{3},h',x}^{*} \right\} \\ + \delta_{n_{1},n_{3}} \bar{\delta}_{n_{1},n_{2}} \delta_{n_{2},n'_{2}} \delta_{n_{1},n'_{1}} \delta_{n_{3},n'_{3}} \mathbb{E} \left\{ a_{n_{2},k,x}^{*} a_{n_{2},k',x} \right\} \\ \cdot \mathbb{E} \left\{ a_{n_{1},h,x} a_{n_{1},l,x} a_{n_{1},h',x}^{*} a_{n_{1},h',x}^{*} a_{n_{1},l',x} \right\} \\ + \delta_{n_{1},n_{2}} \bar{\delta}_{n_{1},n_{3}} \delta_{n_{3},n'_{1}} \delta_{n_{2},n'_{2}} a_{n_{1},n'_{3}} \mathbb{E} \left\{ a_{n_{3},l,x} a_{n_{3},h',x}^{*} \right\} \\ \cdot \mathbb{E} \left\{ a_{n_{1},h,x} a_{n_{1},k,x}^{*} a_{n_{1},h',x} a_{n_{1},h',x}^{*} \right\} \\ \cdot \mathbb{E} \left\{ a_{n_{1},h,x} a_{n_{1},k,x}^{*} a_{n_{1},h',x}^{*} a_{n_{1},h',x}^{*} \right\} \\ \cdot \mathbb{E} \left\{ a_{n_{1},h,x} a_{n_{1},k,x}^{*} a_{n_{1},h',x}^{*} a_{n_{1},h',x}^{*} \right\} \\ \cdot \mathbb{E} \left\{ a_{n_{1},h,x} a_{n_{1},h,x}^{*} a_{n_{1},h',x}^{*} a_{n_{1},h',x}^{*} a_{n_{1},h',x}^{*} \right\} \\ \cdot \mathbb{E} \left\{ a_{n_{1},h,x} a_{n_{1},k,x}^{*} a_{n_{1},h',x}^{*} a_{n_{1},h',x}^{*} a_{n_{1},h',x}^{*} \right\} \\ \cdot \mathbb{E} \left\{ a_{n_{1},h,x}^{*} a_{n_{1},h',x}^{*} a_{n_{1},h',x}^{*} a_{n_{1},h',x}^{*} a_{n_{1},h',x}^{*} \right\} \\ \cdot \mathbb{E} \left\{ a_{n_{1},h,x}^{*} a_{n_{1},h',x}^{*} a_{n_{1},h',x}^{*} a_{n_{1},h',x}^{*} a_{n_{1},h',x}^{*} \right\} \\ \cdot \mathbb{E} \left\{ a_{n_{1},h,x}^{*} a_{n_{1},h',x}^{*} a_{n_{1},h',x}^{*} a_{n_{1},h',x}^{*} a_{n_{1},h',x}^{*} a_{n_{1},h',x}^{*} \right\} \\ \cdot \mathbb{E} \left\{ a_{n_{1},h,x}^{*} a_{n_{1},h',x}^{*} a_$$

in which  $\bar{\delta}_{i,j} = 1 - \delta_{i,j}$ . We can then write this first term of

$$\begin{split} &\sigma_{\text{NLI},n,\mathbf{x},1\text{st}}^{2} = \sum_{n_{1},n_{2},n_{3} \in \mathcal{T}} \delta_{n_{1},n_{3}} \delta_{n_{1},n_{2}} A_{1} + \delta_{n_{2},n_{3}} \bar{\delta}_{n_{1},n_{3}} \\ &\cdot (A_{2} + A_{3}) + \delta_{n_{1},n_{3}} \bar{\delta}_{n_{1},n_{2}} A_{4} + \delta_{n_{1},n_{2}} \bar{\delta}_{n_{1},n_{3}} (A_{5} + A_{6}) \\ &+ \bar{\delta}_{n_{1},n_{2}} \bar{\delta}_{n_{1},n_{3}} \bar{\delta}_{n_{2},n_{3}} (A_{7} + A_{8}), \end{split} \tag{18}$$

where  $A_1, \dots, A_8$  are given in Table IV. Following the same procedure as in [18, Eqs. (27)–(44)] and using (8), we can compute  $A_1$  in (18) (see [18, Eqs. (46)]). Just as the approach employed in [18, Eqs. (48)–(52)], we can evaluate a mix of second and fourth order moments in (18)  $(A_2, \dots, A_6)$  in Table IV). The calculation of a mix of second order moments

<sup>&</sup>lt;sup>3</sup>It is noticeable that without the simplifying assumptions made in [18, Sec. III], quite a few terms must be taken into account for each term of (15), leading to bulky formula.

 $(A_7$  and  $A_8$  in (18)) can be done using [18, Eqs. (40)–(43)]. Looking at the procedure used in [18, Eqs. (48)–(52)], we can also find that  $A_2=A_3,\ A_5=A_6$ , and

$$\sum_{n_1, n_2, n_3 \in \mathcal{T}} \delta_{n_2, n_3} \bar{\delta}_{n_1, n_3} A_2 = \sum_{n_1, n_2, n_3 \in \mathcal{T}} \delta_{n_1, n_2} \bar{\delta}_{n_1, n_3} A_6.$$
(19)

Considering  $A_7 = A_8$  and (19), (18) is equal to

$$\sigma_{\text{NLI},n,\mathbf{x},1\text{st}}^{2} = \frac{64}{81} \sum_{n_{1},n_{2},n_{3} \in \mathcal{T}} P_{n_{1},\mathbf{x}} P_{n_{2},\mathbf{x}} P_{n_{3},\mathbf{x}} \Big( \delta_{n_{1},n_{2}} \\ \cdot \delta_{n_{1},n_{3}} ((\varphi_{1} - 9\varphi_{2} + 12)\chi_{1} + (4\varphi_{2} - 8)\chi_{2} \\ + (\varphi_{2} - 2)\chi_{3} + 2Z) + \delta_{n_{1},n_{3}} \bar{\delta}_{n_{1},n_{2}} ((\varphi_{2} - 2)\chi_{3} + 2Z) \\ + \delta_{n_{1},n_{2}} \bar{\delta}_{n_{1},n_{3}} (2(2\varphi_{2} - 4)\chi_{2} + 4Z) + \bar{\delta}_{n_{1},n_{2}} \bar{\delta}_{n_{1},n_{3}} \bar{\delta}_{n_{2},n_{3}} 2Z \Big),$$

$$(20)$$

where  $\chi_1$ ,  $\chi_2$ ,  $\chi_3$ , and Z are given in Table I, and  $\varphi_1$  and  $\varphi_2$  are expressed in Table II.

We can follow the same approach for the other terms of (15), and so we will not address their detailed derivation and only give their final results. The other terms of (15) can be written as

$$\sigma_{\text{NLI},n,x,2\text{nd}}^{2} = \frac{64}{81} \sum_{n_{1},n_{2},n_{3} \in \mathcal{T}} P_{n_{1},x} P_{n_{2},x} P_{n_{3},x} \Big( \delta_{n_{1},n_{2}} \\ \cdot \delta_{n_{1},n_{3}} ((\varphi_{3} - 4\varphi_{5} - \varphi_{2} + 4)\chi_{1} + (2\varphi_{5} - 2)\chi_{2}) \\ + \delta_{n_{1},n_{2}} \bar{\delta}_{n_{1},n_{3}} 2(\varphi_{5} - 1)\chi_{2} \Big), \tag{21}$$

$$\sigma_{\text{NLI},n,x,3\text{rd}}^{2} = \frac{64}{81} \sum_{n_{1},n_{2},n_{3} \in \mathcal{T}} P_{n_{1},x} P_{n_{2},x} P_{n_{3},x} \Big( \delta_{n_{1},n_{2}} \\ \cdot \delta_{n_{1},n_{3}} ((\varphi_{3} - 4\varphi_{5} - \varphi_{2} + 4)\chi_{1} + (2\varphi_{5} - 2)\chi_{2}) \\ + \delta_{n_{1},n_{2}} \bar{\delta}_{n_{1},n_{3}} (2\varphi_{5} - 2)\chi_{2} \Big), \tag{22}$$

and

$$\sigma_{\text{NLI},n,x,4\text{th}}^{2} = \frac{64}{81} \sum_{n_{1},n_{2},n_{3} \in \mathcal{T}} P_{n_{1},x} P_{n_{2},x} P_{n_{3},x} \Big( \delta_{n_{1},n_{2}} \\ \cdot \delta_{n_{1},n_{3}} ((\varphi_{4} - 4\varphi_{5} - \varphi_{2} + 4)\chi_{1} + (\varphi_{5} + \varphi_{2} - 3)\chi_{2} \\ + (\varphi_{5} - 1)\chi_{3} + Z) \\ + \delta_{n_{1},n_{2}} \bar{\delta}_{n_{1},n_{3}} ((\varphi_{5} + \varphi_{2} - 3)\chi_{2} + 2Z) \\ + \delta_{n_{1},n_{3}} \bar{\delta}_{n_{1},n_{2}} ((\varphi_{5} - 1)\chi_{3} + Z) + \bar{\delta}_{n_{1},n_{2}} \bar{\delta}_{n_{1},n_{3}} \bar{\delta}_{n_{2},n_{3}} Z \Big).$$

By plugging (20), (21), (22), and (23) into (16), we can write (16) as

$$\sigma_{\text{NLI,n,x}}^{2} = \frac{64}{81} \sum_{n_{1},n_{2},n_{3} \in \mathcal{T}} P_{n_{1},x} P_{n_{2},x} P_{n_{3},x} \Big( \delta_{n_{1},n_{2}} \delta_{n_{1},n_{3}} + \frac{1}{2} (\varphi_{1} - 12\varphi_{2} + 2\varphi_{3} + \varphi_{4} - 12\varphi_{5} + 24) \chi_{1} + \frac{1}{2} (\varphi_{2} + 5\varphi_{5} - 15) \chi_{2} + (\varphi_{2} + \varphi_{5} - 3) \chi_{3} + 3Z + \frac{1}{2} (\varphi_{1} + \delta_{n_{1},n_{2}} \bar{\delta}_{n_{1},n_{3}} [(5\varphi_{2} + 5\varphi_{5} - 15) \chi_{2} + 6Z] + \frac{1}{2} (\varphi_{1} + \varphi_{5} - 3) \chi_{3} + 3Z + \frac{1}{2} (\varphi_{1} + \varphi_{5} - 3) \chi_{3} + 2Z + \frac{1}{2} (\varphi_{1} + \varphi_{5} - 3) \chi_{3} + 2Z + \frac{1}{2} (\varphi_{1} + \varphi_{1} - 2) \chi_{3} + 2Z + \frac{1}{2} (\varphi_{1} + \varphi_{1} - 2) \chi_{3} + 2Z + \frac{1}{2} (\varphi_{1} + \varphi_{1} - 2) \chi_{3} + 2Z + \frac{1}{2} (\varphi_{1} + 2) \chi_{3} + 2Z + 2Z$$

Using the fact that  $\bar{\delta}_{i,j} = 1 - \delta_{i,j}$ , (24) is expressed as (11).

### REFERENCES

- R.-J. Essiambre, G. Kramer, P. J. Winzer, G. J. Foschini, and B. Goebel, "Capacity limits of optical fiber networks," *J. Lightw. Technol.*, vol. 28, no. 4, pp. 662–701, Feb. 2010.
- [2] E. Agrell and M. Karlsson, "Power-efficient modulation formats in coherent transmission systems," *J. Lightw. Technol.*, vol. 27, no. 22, pp. 5115–5126, Nov. 2009.
- [3] M. Karlsson and E. Agrell, "Which is the most power-efficient modulation format in optical links?" Opt. Express, vol. 17, no. 13, pp. 10814– 10819, June 2009.
- [4] A. Carena, V. Curri, G. Bosco, P. Poggiolini, and F. Forghieri, "Modeling of the impact of nonlinear propagation effects in uncompensated optical coherent transmission links," *J. Lightw. Technol.*, vol. 30, no. 10, pp. 1524–1539, May 2012.
- [5] A. Mecozzi and F. Matera, "Polarization scattering by intra-channel collisions," Opt. Express, vol. 20, no. 2, pp. 1213–1218, Jan. 2012.
- [6] P. Johannisson and M. Karlsson, "Perturbation analysis of nonlinear propagation in a strongly dispersive optical communication system," *J. Lightw. Technol.*, vol. 31, no. 8, pp. 1273–1282, Apr. 2013.
- [7] R. Dar, M. Feder, A. Mecozzi, and M. Shtaif, "Properties of nonlinear noise in long, dispersion-uncompensated fiber links," *Opt. Express*, vol. 21, no. 22, pp. 25 685–25 699, Nov. 2013.
- [8] V. Curri, A. Carena, P. Poggiolini, G. Bosco, and F. Forghieri, "Extension and validation of the GN model for non-linear interference to uncompensated links using Raman amplification." *Opt. Express*, vol. 21, no. 3, pp. 3308–17, Feb. 2013.
- [9] A. Carena, G. Bosco, V. Curri, Y. Jiang, P. Poggiolini, and F. Forghieri, "EGN model of non-linear fiber propagation," *Opt. Express*, vol. 22, no. 13, pp. 16335–16362, June 2014.
- [10] A. Splett, C. Kurtzke, and K. Petermann, "Ultimate transmission capacity of amplified optical fiber communication systems taking into account fiber nonlinearities," in *Proc. European Conf. Optical Communication*, Montreux, Switzerland, Sep. 1993.
- [11] K. Peddanarappagari and M. Brandt-Pearce, "Volterra series transfer function of single-mode fibers," *J. Lightw. Technol.*, vol. 15, no. 12, pp. 2232–2241, Dec. 1997.
- [12] A. Carena, V. Curri, G. Bosco, P. Poggiolini, and F. Forghieri, "Modeling of the impact of nonlinear propagation effects in uncompensated optical coherent transmission links," *J. Lightw. Technol.*, vol. 30, no. 10, pp. 1524–1539, May 2012.
- [13] L. Beygi, E. Agrell, P. Johannisson, M. Karlsson, and H. Wymeersch, "A discrete-time model for uncompensated single-channel fiber-optical links," *IEEE Trans. Commun.*, vol. 60, no. 11, pp. 3440–3450, Nov. 2012.
- [14] A. Mecozzi and R. J. Essiambre, "Nonlinear Shannon limit in pseudolinear coherent systems," *J. Lightw. Technol.*, vol. 30, no. 12, pp. 2011–2024, June 2012.
- [15] E. Agrell, G. Durisi, and P. Johannisson, "Information-theory-friendly models for fiber-optic channels: A primer," in *IEEE Information Theory Workshop (ITW)*, Jerusalem, Israel, Apr.-May 2015.
- [16] H. Rabbani, G. Liga, V. Oliari, L. Beygi, E. Agrell, M. Karlsson, and A. Alvarado, "A general analytical model of nonlinear fiber propagation in the presence of Kerr nonlinearity and stimulated Raman scattering," arXiv preprint arXiv:1909.08714v2, June 2020.
- [17] G. Liga, A. Barreiro, H. Rabbani, and A. Alvarado, "Extending fibre nonlinear interference power modelling to account for general dualpolarisation 4D modulation formats," *Entropy*, vol. 22, no. 11, p. 1324, Nov. 2020.
- [18] H. Rabbani, M. Ayaz, L. Beygi, G. Liga, A. Alvarado, E. Agrell, and M. Karlsson, "Analytical modeling of nonlinear fiber propagation for four dimensional symmetric constellations," *J. Lightw. Technol.*, vol. 39, no. 9, pp. 2704–2713, May 2021.
- [19] O. Golani, R. Dar, M. Feder, A. Mecozzi, and M. Shtaif, "Modeling the bit-error-rate performance of nonlinear fiber-optic systems," *J. Lightw. Technol.*, vol. 34, no. 15, pp. 3482–3489, Aug. 2016.
- [20] R. Dar, M. Feder, A. Mecozzi, and M. Shtaif, "Inter-channel nonlinear interference noise in WDM systems: Modeling and mitigation," *J. Lightw. Technol.*, vol. 33, no. 5, pp. 1044–1053, Mar. 2015.
- [21] E. Agrell, "Database of sphere packings," 2016. [Online]. Available: http://codes.se/packings/.

[22] P. Poggiolini, A. Nespola, Y. Jiang, G. Bosco, A. Carena, L. Bertignono, S. M. Bilal, S. Abrate, and F. Forghieri, "Analytical and experimental results on system maximum reach increase through symbol rate optimization," *J. Lightw. Technol.*, vol. 34, no. 8, pp. 1872–1885, Apr. 2016.

- [23] M. Sjodin, E. Agrell, and M. Karlsson, "Subset-optimized polarization-multiplexed PSK for fiber-optic communications," *IEEE Commun. Lett.*, vol. 17, no. 5, pp. 838–840, May 2013.
- [24] T. A. Eriksson, S. Alreesh, C. Schmidt-Langhorst, F. Frey, P. W. Berenguer, C. Schubert, J. K. Fischer, P. A. Andrekson, M. Karlsson, and E. Agrell, "Experimental investigation of a four-dimensional 256-ary lattice-based modulation format," in *Proc. Optical Fiber Communication Conf.*, Los Angeles, CA, USA, Mar. 2015.
- [25] I. Roberts, J. M. Kahn, and D. Boertjes, "Convex channel power optimization in nonlinear WDM systems using Gaussian noise model," *J. Lightw. Technol.*, vol. 34, no. 13, pp. 3212–3222, July 2016.
- [26] P. Poggiolini, G. Bosco, A. Carena, V. Curri, Y. Jiang, and F. Forghieri, "A detailed analytical derivation of the GN model of non-linear interference in coherent optical transmission systems," arXiv preprint arXiv:1209.0394, June 2014.